Journal of Fluorescence (2019) 29:711–717
https://doi.org/10.1007/s10895-019-02380-6

ORIGINAL ARTICLE

Beacons Contribute Valuable Empirical Information to Theoretical 3-D Aptamer-Peptide Binding

John G. Bruno [1,2] · Taylor Phillips [1]

Received: 4 January 2019 / Accepted: 17 April 2019 / Published online: 1 May 2019

Abstract
DNA aptamers were developed against five different peptides from the known binding regions of anti-Cytomegalovirus and anti-Herpes Simplex Virus-2 antibodies and the aptamers were ranked by relative affinity based on an ELISA-like (ELASA) microplate assay. The secondary structures of the top five highest affinity aptamers were studied for stem-loop commonalities and the most probable peptide binding sites. Two of these stem-loop structures were converted into beacons by addition of TYE 665 dye on the 5′ end and Iowa Black quencher on the 3′ end. When competed against increasing concentrations of each of the five peptides, only three of the possible ten interactions demonstrated "lights on" fluorescence beacon responses. When modeled by generation of PDB files, after passage through PATCHDOCK and YASARA, two of the aptamer beacon-peptide interactions showed no theoretical evidence of separating the G-C stem-loop region, despite clear empirical evidence of separation of the fluorophore and quencher beyond the Förster distance leading to abundant fluorescence. And in the second beacon's case, YASARA modeling suggested that the beacon was always open despite clear empirical evidence that it was not (no fluorescence response) and only opened in the presence of one of the five peptides. These results are interpreted as a demonstration that 3-dimensional docking software such as PATCHDOCK and YASARA, which are based on rigid receptor-ligand shape complementarity may not reflect the "induced-fit" interactions between aptamers and their cognate targets. Therefore, for the most complete and accurate picture of aptamer-peptide binding, several theoretical and empirical (e.g., beacon fluorescence) analysis methods may be needed.

Keywords Aptamer · Beacon · Fluorescence · Induced-fit · PATCHDOCK · Stem-loop · YASARA

Introduction

Cytomegalovirus (CMV) and Herpes Simplex Virus Type 2 (HSV-2) are common viruses posing a significant risk of congenital infection to neonates. For example, the WHO estimates that 417 million people aged 15–49 (11%) worldwide have HSV-2 infection which is lifelong and can affect infants via disseminated disease, skin, ocular and oral disease or central nervous system infection. Efforts to develop effective vaccines to these viruses are hampered by an inability to rapidly identify seronegative female test subjects of child-bearing age. DNA aptamers developed against such antibodies could be used to identify anyone in the general public who has been exposed (seroconverted) to CMV or HSV-2. Therefore, an attempt was made to develop anti-idiotypic aptamers against the binding regions of antibodies induced by CMV and HSV-2 infection. Such aptamers could rapidly identify seronegative and seropositive test subjects to enroll in or reject from clinical vaccine trials, especially if their binding pockets were converted into rapid response and facile "lights on" fluorescent beacons.

In the present work, aptamers were developed against four consensus peptides (11–13 amino acids in length) from the accessible Complementarity Determining Regions (CDR) or binding regions of human anti-CMV and anti-HSV-2 antibodies as defined by Spindler et al. [1] for anti-CMV and Bugli et al. [2] for anti-HSV-2 antibodies. These target peptide amino acid sequences are listed in Table 1. Sixty-five unique aptamer DNA sequences of 100 bases in length were

✉ John G. Bruno
jbruno@nanohmics.com

[1] Operational Technologies Corporation, 4100 NW Loop 410, Suite 230, San Antonio, TX 78229, USA

[2] Nanohmics, Inc., 6201 E. Oltorf Street, Suite 400, Austin, TX 78741, USA

Table 1 Amino acid sequences of the target peptides

Peptide	AA sequence
CMV-1	KTV**SN**SGLSLLYY
CMV-2	KT**M**TTSGLSLLYY
CMV-3	KTVTT**F**G**A**SLLYY
CMV-4	KTVTTSG**M**SLLYY
HSV-2	**RRKSCIGGSCR**

Unique non-homologous amino acids in each peptide are bolded

generated against the collection of five different peptides conjugated to magnetic microbeads by Systematic Evolution of Ligands by EXponential enrichment (SELEX) [3, 4] and studied for primary sequence (Table 2) and secondary stem-loop commonalities that led to the selection of two loops for development as aptamer beacons [4]. The two different aptamer beacons (Table 2) were tested against varied concentrations of the five peptides and certified CMV-exposed (seroconverted or CMV antibody positive) and unexposed pooled human sera with the results reported herein. In addition, the aptamer-peptide interactions were modeled in 3-D using PATCHDOCK [5] and YASARA [6–9] with some results that contradicted the aptamer beacon-peptide fluorescence titration analyses. Reasons for the theoretical versus empirical data contradictions are discussed.

Materials and Methods

Materials

The five peptides listed in Table 1 were obtained from GenWay Biotech, Inc. (San Diego, CA) at 98% purity. All DNA primers, SELEX aptamer templates, biotinylated aptamer candidates and beacons (Table 2) were purchased from Integrated DNA Technologies, Inc. (Coralville, IA). CMV antibody positive and negative human sera samples were purchased from BioCollections Worldwide, Inc. (Miami, FL) and certified by a variety of assays including the Abbott Axsym CMV IgG, Bio-Rad CMV IgG ELISA and Diamedix CMV IgG tests.

SELEX Aptamer Selection and Development

One hundred μg of each of the peptides was dissolved in 1 ml of sterile phosphate buffered saline (PBS, pH 7.2) and separately immobilized on 100 μl of stock 2.8 μm Dynal (M280) tosyl coated-magnetic beads (MBs, Invitrogen Corp., Carlsbad, CA) for 2 h at 37 °C. Peptide-conjugated MBs were then collected using a Dynal MPC-S magnetic rack and washed three times in 1 mL of sterile PBS. Peptide-MBs were next blocked for 2 h at 37 °C in sterile PBS plus 2% ethanolamine and washed three times as before in 1 ml aliquots of sterile PBS. DNA aptamers were developed against each of the peptide-conjugated MBs through ten rounds of selection and PCR amplification as previously described in the literature [3, 4]. The presence of 100 bp aptamer PCR products were verified after each round of selection by ethidium bromide-stained 2% agarose gel electrophoresis against standard DNA ladders. Aptamers from the tenth round of selection and amplification were cloned into chemically competent *E. coli* using a Lucigen GC kit (Middleton, WI). All aptamers were sequenced by rolling circle amplification dideoxynucleotide methodology with proprietary treatment for high GC content DNA sequencing at Sequetech Corp. (Mountain View, CA).

ELASA Microplate Assays

Enzyme-Linked Aptamer Sorbent Assay (ELASA) screening to identify and rank the highest affinity and most specific aptamer candidates was conducted by using N-oxy-

Table 2 DNA sequences of the top CMV anti-idiotypic aptamers and their derived beacons

Aptamer	DNA sequence
CMV1-4R	ATCCGTCACACCTGCTCTAGACCATTCTGTTATTGCTTCTCTCCATAAGGTCCT GGCCTAGTCAAGGGGCCTAGACAGCGCGTGGTGTTGGCTCCCGTAT
CMV1-12R	ATCCGTCACACCTGCTCTCGTTAACTCGGACATCGACAGACTCAACGGTGGC GGCGGGTCTGGTGCGCACGGGGCGGGTAGGTGGTGTTGGCTCCCGTAT
CMV3-4F	ATACGGGAGCCAACACCACCACGTCCACCCTGCGCGTCCGGTGTTATGCA TCGGGAACTTGTAGCAGTCTTCAGGGGAGGGGAGAGCAGGTGTGACGGAT
CMV3-15R	ATCCGTCACACCTGCTCTACACAACAAAGCGCGTCGTTTCAGTTGGCTAA TTTGATTCGGCGTGTCGAGCTCGTATGGTTTGTGGTGTTGGCTCCCGTAT
CMV4-12F	ATACGGGAGCCAACACCACCTCAACCACGTCCCTAATCCAACATCAGTTA ATGAATCTTCATCACGTTCTCACACCCCACTACAGAGCAGGTGTGACGGAT
Beacon	DNA sequence
A11	CGGTGGCG
E7	CGAGCTCG

All DNA sequences are presented 5′ to 3′ from left to right

succinimde (NOS)-coated Corning CoStar Cat. No. 2525 microplates in which the peptides were tethered to the plate bottom at the N-terminus or at lysines in their structures (Table 1). A microplate containing 4 nanomoles of each of the 65 different lyophilized aptamer candidates having 5′-biotin linkers was obtained from Integrated DNA Technologies. Wells were rehydrated in 250 μl of sterile PBS and used at 0.8 nanomoles (50 μl) of each 5′-biotinylated aptamer per well for ELASA. The 5′-biotinylated candidate aptamers were added to the NOS plate containing the immobilized peptides and gently swirled for 30 min at room temperature (~ 25 °C) and then decanted. The plates were washed once in 200 μl of sterile PBS per well for 5 min and decanted again. Then 100 μl of 1:2000 diluted streptavidin-peroxidase conjugate (Invitrogen, Cat. No S911) from a 1 mg/ml stock in PBS stored at 4 °C was added per well and the plates were again swirled for 15 min at room temperature. Plates were decanted and washed in 200 μl of PBS plus 0.01% Tween 20 for 5 min, followed by decanting and a final rinse with 200 μl per well of sterile PBS. After decanting, 100 μl of One-Step® ABTS (Kirkegaard Perry Labs, Gaithersburg, MD) was added per well and wells were allowed to develop until at least one well achieved an absorbance of ~ 1.0 at 405 nm using a microplate reader.

Secondary Structural Analyses and Beacon Selection

Secondary structural analyses were conducted using UNAFold and Vienna RNA software to ensure the most accurate 2-D aptamer structures. For the data shown in Fig. 1, the top five highest affinity aptamer candidates were subjected to free internet UNAFold software (URL: http://www.idtdna.com/UNAFold) with temperature set at 25 °C and the ionic strength at 145 mM sodium (approximate physiologic salt concentration). The top secondary structures based on the greatest negative ΔG for each aptamer are shown in Fig. 1. For the secondary stem-loop structures given in Fig. 2, the same top 5 aptamer candidate DNA sequences were subjected to free Vienna RNA software (http://rna.tbi.univie.ac.at/cgi-bin/RNAWebSuite/RNAfold.cgi) on the webserver [10] using a temperature of 25 °C and the 2004 Matthews model DNA parameter settings.

Aptamer Beacon Fluorescence Assessment

Two aptamer beacons were selected and designated A11 and E7 based on their position in the final ELASA microplate test. These beacons were purchased from Integrated DNA Technologies with 5'-TYE 665 and 3'-Iowa Black quencher modifications (0.18 mg yield for each) and rehydrated in 1 ml of sterile PBS. The beacons were then diluted to 360 ml each in PBS (final concentrations equal 500 ng/ml). Next, a series of two-fold serial dilutions of each CMV or HSV2 peptide was made beginning with 200,000 ng/ml of peptide down to 22.5 ng/ml and a baseline PBS blank. Two ml of each separate beacon (1000 ng final beacon amount per cuvette) were added on top of the 1 ml peptide dilutions in the cuvettes which were capped and mixed thoroughly for 15 min at room temperature. The cuvettes were then placed in a Cary-Varian Eclipse™ spectrofluorometer and fluorescence spectra were acquired using an excitation of 645 nm and scanning emissions from 650 to 700 nm using a photomultiplier tube (PMT) voltage setting of 1000 V.

3-Dimensional Molecular Docking Models

The basic protocol for generating and docking 3-D aptamer stem-loop plus peptide ligand complexes by sequentially stringing together various webserver software has already been described by Bruno [8]. Briefly, to start the process, Vienna RNAFold webserver [10] was employed with the advanced option using the 2004 Mathews model DNA

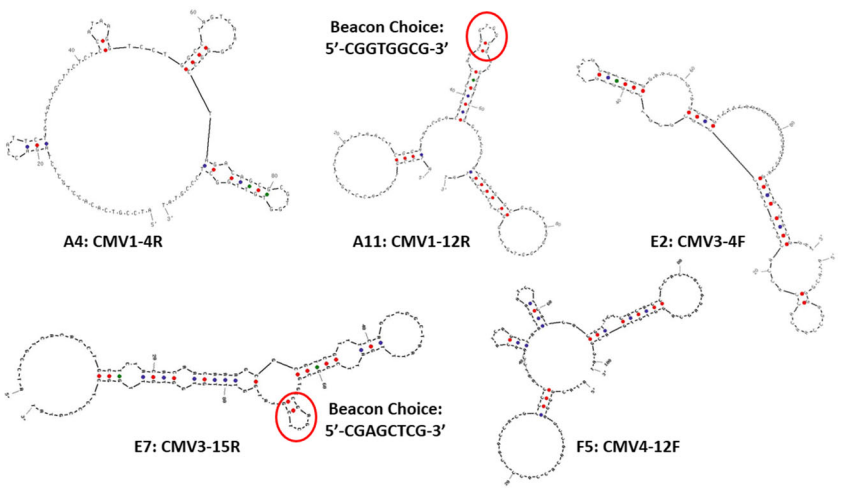

Fig. 1 Secondary stem-loop structures of the top 5 highest affinity DNA aptamers against the various CMV antibody peptides as determined by UNAFold software using room temperature (25 °C). Notations are shown as ELASA microwell number: aptamer name. Well numbers (e.g., A11 or E7) were later used to identify beacon candidates (circled stem-loop structures)

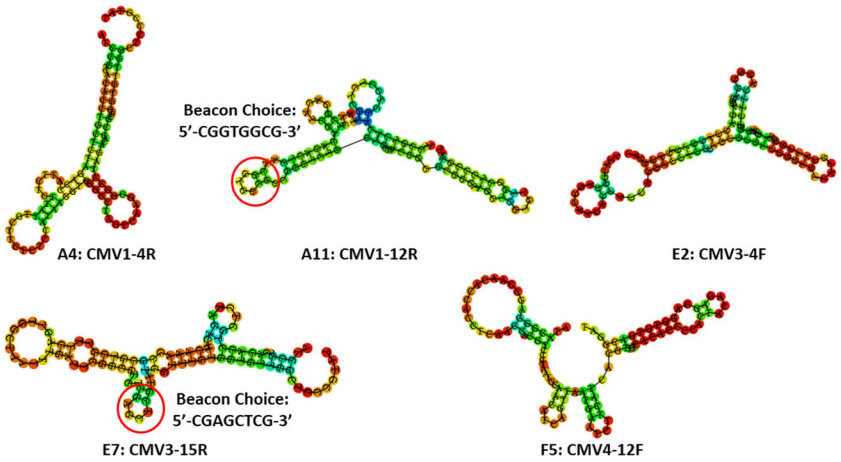

Fig. 2 Secondary stem-loop structures of the top 5 highest affinity DNA aptamers against the various CMV antibody peptides as determined by Vienna RNA software using DNA parameters at 25 °C and physiologic sodium concentration (145 mM). Notations are shown as ELASA microwell number: aptamer name. Well numbers (e.g., A11 or E7) were later used to identify beacon candidates. Note that the circled beacon choices based on Vienna RNA software agreed with the UNAFold results circled in Fig. 1

parameters for the aptamer beacon stem-loop structures (Table 2 bottom). Vienna RNA output dot-bracket notation data for each of the beacons which were then input to the RNA Composer webserver [11] (http://rnacomposer.cs.put.poznan.pl/) to generate the top PDB files containing 3-D structures of the aptamer beacons without the fluorophore or quencher ends. Each of the five peptides from Table 1 were entered into the Pep-Fold 2.0 webserver (http://bioserv.rpbs.univ-paris-diderot.fr/services/PEP-FOLD/) to generate PDB files of the top 3-D peptide structures. Next, the aptamer beacons were entered into the PATCHDOCK [5] rigid shape complementarity webserver (https://bioinfo3d.cs.tau.ac.il/PatchDock/) as receptors along with each of the five peptides as individual ligands to yield PDB files of all the various possible beacon-peptide complexes. The PDB aptamer beacon-peptide complex PDB files were then visualized in 3-D using downloaded Yet Another Scientific Artificial Reality Application (YASARA; http://www.yasara.org/downloads.htm) software.

Results and Discussion

Both web-based 2-D DNA structural software packages (UNAFold and Vienna RNA) produced similar, albeit somewhat different, results as evident when Figs. 1 and 2 are compared. But, both software packages yielded identical small loop structures which were chosen to be the A11 and E7 beacons. The authors considered single-stranded (ss) loop structures to be likely binding sites because peptide binding to such ss regions would not require a large input of free energy to break any hydrogen bonds in double-stranded (ds) regions (i.e., ss regions are easily accessed). Furthermore, the positioning of loop structures in the mid-sections of each of the five aptamer candidates was considered to be important binding site selection factor, because these ss loops were central in the aptamers and distal from the constant PCR primer ends of each aptamer. Similarities in the central loops (more likely binding pockets) yielded two potential loop sequences which stood out in the two highest affinity aptamers (circled in Figs. 1 and 2). These were designated A11 and E7 to indicate the microwells from which they originated in ELASA. These short oligonucleotide sequences were then synthesized at Integrated DNA Technologies with 5'-TYE 665 fluorescent dye and 3'-Iowa Black RQ quencher and purified by HPLC. These molecular beacon DNA sequences were: A11: 5'-CGGTGGCG-3′ and E7: 5'-CGAGCTCG-3′. While quite short, the fact that these 8-base sequences formed true stem-loop beacon structures in solution is supported by the secondary structures circled in Figs. 1 and 2 as well as the very low baseline (quenched) fluorescence observed for all of the blanks (red spectral traces of the aptamer beacons alone without target peptides) in the 10 experiments illustrated in Fig. 3.

Results in Fig. 3 show that a mild FRET response with the A11 aptamer beacon candidate was observed when PBS buffer dilutions of the CMV-1 peptide were used (some separation of emission spectra in panel A based on increasing peptide concentration), but a very robust FRET response was seen with the CMV-3 peptide dilutions (Fig. 3c). No FRET responses between the A11 beacon and the CMV-2, CMV-4 or HSV-2 peptides were noted which speaks to the specificity of the A11 beacon candidate (a putative CMV antibody aptamer binding site). For the E7 aptamer beacon candidate, only the CMV-3 peptide elicited a "lights on" fluorescence response as a function of peptide concentration (Fig. 3h). The complete lack of a fluorescence response in Fig. 3 panels b, d, e, f, g, i and j speaks again to the specificity of the A11 and E7 aptamer beacons for the CMV-3 peptide with some specificity apparently existing between the A11 beacon and the CMV-1 peptide. As further controls (not shown), we also evaluated the fluorescence of each of the target peptides in PBS by themselves to be certain that the increasing fluorescence as a function of peptide concentration for the CMV-3 peptide (Fig. 3c and h) was not due to peptide autofluorescence. As the reader can see from Table 1, the CMV peptides are highly related in terms of amino acid composition and

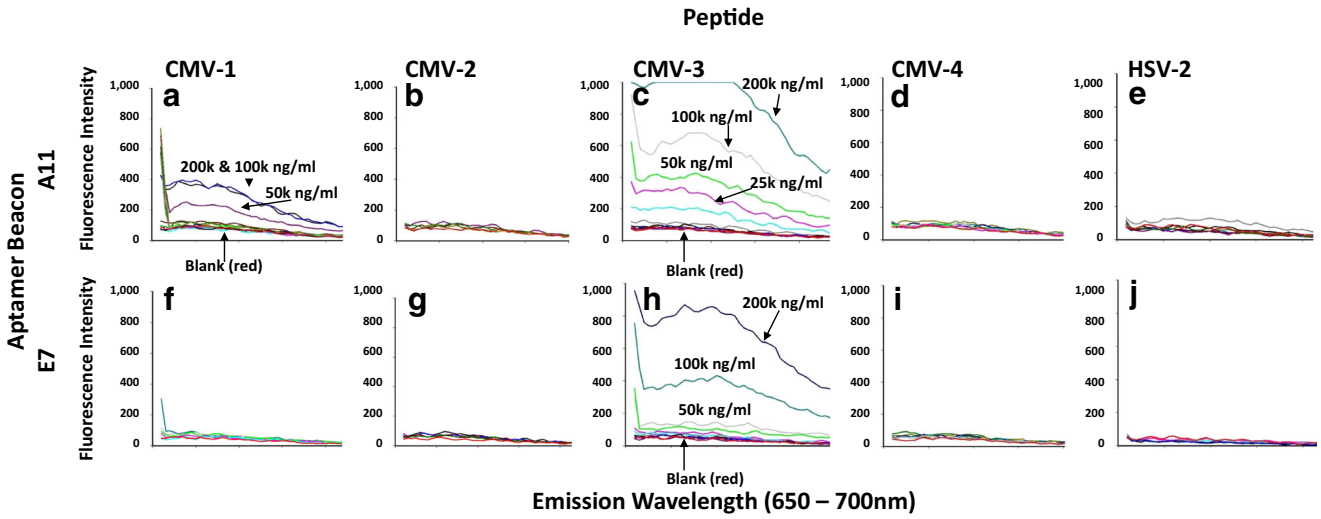

Fig. 3 Fluorescence responses of each of the aptamer beacons (A11 and E7) versus the five peptides with peptide concentrations varied from 200,000 ng/ml to 22.5 ng/ml with a zero peptide baseline spectral trace (red trace) in each panel. Note the very strong "lights on" fluorescence response by both aptamer beacons as a function of CMV-3 peptide level (panels **c** and **h**). Some of the peptide concentrations are labeled and indicated by arrows for reference in the otherwise tightly clustered spectra arising from interaction of the beacons with the various peptide concentrations. In general, the spectral intensity followed a function of peptide concentration (panels **a**, **c** and **h**), if a fluorescence response was observed at all

none of the peptides autofluoresced significantly in the red region of the spectrum (e.g., 650–700 nm) where the Fig. 3 data was collected despite some low level autofluorescence in the blue-green region where most peptides and proteins may autofluoresce (data not shown for brevity).

While the results in Fig. 3 were encouraging for detection of CMV-3 peptide and possibly some anti-CMV antibodies in buffer, the same aptamer beacon systems (A11 and E7) failed to detect CMV antibodies in pooled human sera as shown in Fig. 4. The failure was not due to lack of a fluorescence response, but rather as illustrated in Fig. 4, both CMV antibody positive and CMV antibody negative pooled sera gave roughly equivalent "lights on" beacon fluorescence responses to various dilutions of the pooled sera, suggesting that the beacons

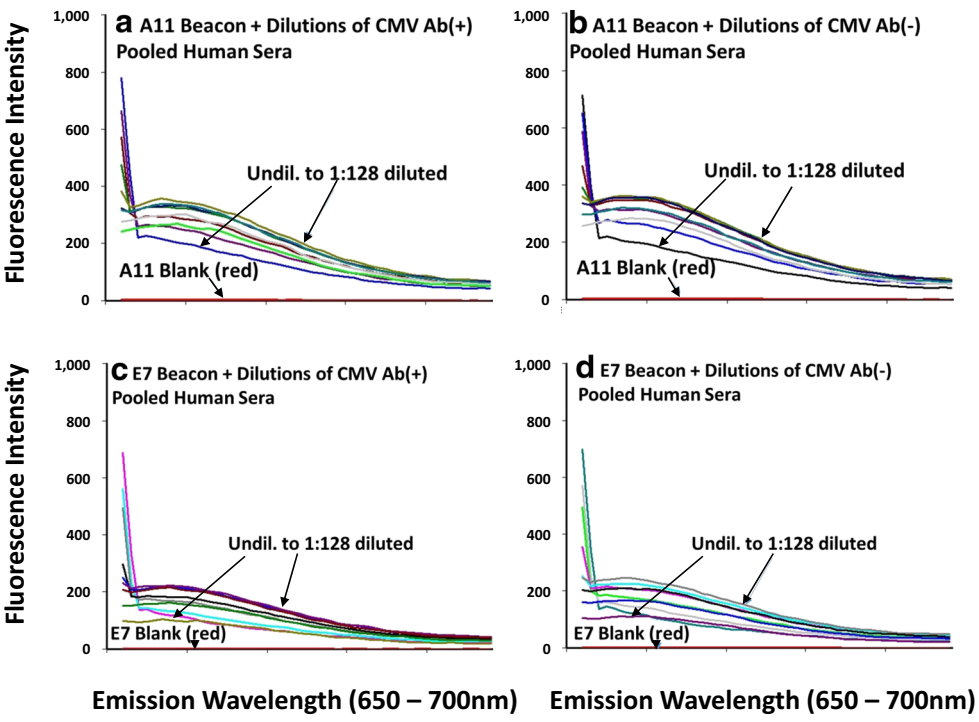

Fig. 4 Comparison of aptamer beacon fluorescence responses for the A11 and E7 aptamer beacons to undiluted and serial two-fold dilutions of confirmed and pooled CMV antibody (Ab) positive (+) and Ab negative (−) human sera obtained from BioCollections Worldwide. Note the approximately equal fluorescence responses of both beacons to the serum dilutions regardless of their CMV antibody status (+ or -), indicating a lack of specificity of the aptamer beacons for CMV antibodies in human serum. The spectra representing undiluted serum and the 1:128 serum dilutions are indicated by arrows for reference in the otherwise tightly clustered spectra arising from interaction of the beacons with the various serum dilutions

were nonspecifically "opening" (separating the fluorophore and quencher at the ends of double-stranded stem regions) in response to something else in serum beside the CMV-3 peptide in CMV antibodies. Or perhaps the CMV-3 peptide is common in many antibodies or other serum proteins, thus leading to the nonspecific response. In retrospect, the aptamers against peptide-conjugated magnetic beads probably should have been selected in diluted human serum to eliminate any serum cross-reactive aptamers. While it is possible that some of the fluorescence increases observed in the Fig. 4 experiments could be due to serum nuclease degradation of the aptamer beacons, thus liberating unquenched TYE 665 fluorophores, the effect of serum nucleases during the 15 assay incubation period would likely be minimal in such a brief timeframe. In addition, if serum nucleases were a major contributor to the fluorescence increases seen in Fig. 4, then the undiluted serum spectra would be expected to be stronger than the 1:128 diluted sample spectra, but this is not observed in any of the four experiments depicted in Fig. 4 (compared spectra pointed to by the arrows in each panel).

On a more general or fundamental level, however, we were interested in comparing the empirical aptamer beacon fluorescence results from Fig. 3 with theoretical docking models generated by YASARA. However, as Fig. 5a demonstrates, the combination of PATCHDOCK and YASARA analyses showed no evidence of the G-C bonds in the A11 beacon being separated in response to docking with the CMV-3 peptide. But, clearly this "induced-fit" occurs in reality as evidenced by Fig. 3c. Likewise, some separation of the A11 beacon stem region occurs in response to binding the CMV-1 peptide as shown in Fig. 3a. Examination of Table 1 shows that CMV-1 and CMV-3 peptides differ by just a few amino acids and suggests that the F (phenylalanine) amino acid in the CMV-3 peptide may be responsible for the strong beacon response seen in Fig. 3c and h, although this is not seen in Fig. 5 or with any of the beacon-peptide PATCHDOCK and YASARA generated 3-D complexes (images not shown for brevity). Oddly too, the E7 beacon always appeared to be linearized and therefore opened in all of the PATCHDOCK plus YASARA simulations (e.g., Fig. 5b), but Fig. 3 (panels f, g, i and j) strongly suggest that the E7 stem region remained closed (double-stranded) in the presence of four of the five peptides except for CMV-3 (Fig. 3h).

One caveat and potential deficiency in the 3-D modeling method presented here is that RNA Composer outputs PDB files for RNA, not DNA. Although RNA Composer will accept DNA input data, it converts all thymines (Ts) to uridines (Us) in its PDB output files. For 3-D DNA aptamer structure modeling, the Us can be converted back to Ts using Discovery Studio Visualizer [8]. Unfortunately, the authors did not have access to this software and there is only one T near the middle regions of either aptamer beacon (Table 1). Hence, the substitution of a single U and the difference of a few hydroxyl groups on the sugar moieties that rarely participate in aptamer-ligand binding in each beacon were not considered to be major factors in the 3-D docking models. And ultimately, the main thesis of this work is that PATCHDOCK and YASARA, despite all of their shape complementarity and docking analysis abilities, cannot detect the "induced-fit" of ds aptamer beacon stem regions that are being unzipped (verified by Fig. 3a, c and h), but not predicted in Fig. 5a. Hence, the core message or lesson from this work is centered on the ds stem regions of the aptamer beacons which are consistent, stable and fixed (Figs. 1 and 2) whether modeled

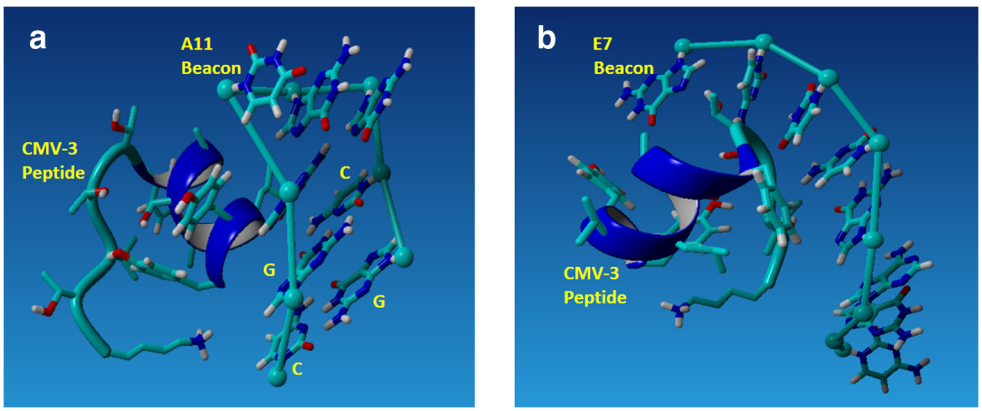

Fig. 5 Representative docked YASARA images of (**a**) the A11 beacon docked with the CMV-3 peptide and (**b**) the E7 beacon with the CMV-3 peptide. Neither beacon is shown with its TYE 665 or Iowa Black end labels. Note in panel **a** that the G-C double-stranded stem region remains closed despite the empirical fluorescence evidence of it opening in Fig. 3c. Note also in Fig. 5b, that the E7 beacon is fully opened which is supported by empirical fluorescence evidence in Fig. 3h. However, the E7 beacon always appeared wide open regardless of the peptide that it was interacting with (images not all shown for brevity) which contradicts the lack of a fluorescence response in Fig. 3f, g, i and j which demonstrate that the E7 beacon's end is actually closed in reality and has an intact double-stranded stem region even when bound to the CMV-1, -2, -4 and HSV-2 peptides. The lack of ability of PATCHDOCK and YASARA to illustrate any induced-fit in the stem region by the CMV-3 peptide with the A11 beacons, which is clearly real from Fig. 3c, is attributed to these programs emphasizing rigid shape complementarity docking between receptors (aptamer beacons) and ligands (peptides) and not taking into account induced-fit modes based on minimized free energy in the bound complexes

as DNA or RNA. For larger aptamer-ligand 3-D models, readers are advised to use Discovery Studio Visualizer after generating the aptamer PDB file by RNA Composer to convert RNA features to DNA for optimal 3-D accuracy if needed, but for the 8-base DNA beacons examined for induced-fit unzipping of G-C hydrogen bonds in ds beacon stem regions herein, the impact of modeling the beacons as RNA instead of DNA oligonucleotides was probably minimal.

Conclusion

The present work illustrates that while it is quite possible to generate very strong aptamer beacon fluorescence responses and assays against key peptides, these reagents may not demonstrate specificity in serum unless the aptamers are adsorbed against serum proteins during aptamer development. This work also demonstrates that it is possible to develop 3-D aptamer stem-loop-peptide docking models with freely available software and webservers such as Vienna RNA, RNA composer, PATCHDOCK and YASARA, but such models are based on rigid shape complementarity and do not account for induced-fit into the ds hydrogen-bonded G-C stem regions of aptamers. Therefore, to gain a clearer 3-D image of aptamer-peptide binding, tools such as aptamer beacons may be helpful to verify if hydrogen bonds in the stem regions are being forced open upon target binding.

Acknowledgements Work was funded by NIH SBIR contract no. HHSN272201700075C.

Author's Contributions JB conceived all experiments, conducted the fluorescence experiments and 3-D modeling, and wrote the manuscript. TP developed and screened the aptamers by ELASA and edited the manuscript.

Compliance with Ethical Standards

Conflict of Interests The authors declare no conflict of interest or competing interests.

References

1. Spindler N, Diestel U, Stump JD, Wiegers AK, Winkler TH, Sticht H, Mach M, Muller YA (2014) Structural basis for the recognition of human Cytomegalovirus glycoprotein B by a neutralizing human antibody. PLoS Pathog 10:e1004377
2. Bugli F, Manzara S, Torelli R, Graffeo R, Santangelo R, Cattani P, Fadda G (2004) Human monoclonal antibody fragment specific for glycoprotein G in herpes simplex virus type 2 with applications for serotype-specific diagnosis. J Clin Microbiol 42:1250–1253
3. Bruno JG, Richarte AM, Phillips T (2014) Preliminary development of a DNA aptamer-magnetic bead capture electrochemiluminescence sandwich assay for brain natriuretic peptide. Microchem J 115: 32–38
4. Bruno JG, Carrillo MP, Phillips T, Hanson D, Bohmann JA (2011) DNA aptamer beacon assay for C-telopeptide and handheld fluorometer to monitor bone resorption. J Fluoresc 21:2021–2033
5. Schneidman-Duhovny D, Inbar Y, Nussinov R, Wolfson HJ (2005) PatchDock and SymmDock: servers for rigid and symmetric docking. Nucleic Acids Res 33:W363–W367
6. Albada HB, Golub E, Willner I (2015) Computational docking simulations of a DNA-aptamer for argininamide and related ligands. J Comput Aided Mol Des 29(7):643–654. https://doi.org/10.1007/s10822-015-9844-5
7. Ahirwar R, Nahar S, Aggarwal S, Ramachandran S, Maiti S, Nahar P (2016) In silico selection of an aptamer to estrogen receptor alpha using computational docking employing estrogen response elements as aptamer-alike molecules. Sci Rep 6: 21285. https://doi.org/10.1038/srep21285
8. Bruno JG (2017) Do it yourself 3-dimensional aptamer-ligand molecular modeling. J Bionanosci 11:183–186. https://doi.org/10.1166/jbns.2017.1437
9. Jeddi I, Saiz L (2017) Three-dimensional modeling of single stranded DNA hairpins for aptamer-based biosensors. Sci Rep 7:1178. https://doi.org/10.1038/s41598-017-01348-5
10. Hofacker IL (2003) Vienna RNA secondary structure server. Nucleic Acids Res 31(13):3429–3431
11. Popenda M, Szachniuk M, Antczak M, Purzycka KJ, Lukasiak P, Bartol N, Blazewicz J, Adamiak RW (2012) Automated 3D structure composition for large RNAs. Nucleic Acids Res 40(14):e112. https://doi.org/10.1093/nar/gks339